Monitoring wine fermentation deviations using an ATR-MIR spectrometer and MSPC charts

Julieta Cavaglia[a], Daniel Schorn-García[a], Barbara Giussani[b], Joan Ferré[c], Olga Busto[a], Laura Aceña[a], Montserrat Mestres[a], Ricard Boqué[c(*)]

a. Universitat Rovira i Virgili. Instrumental Sensometry (iSens), Department of Analytical Chemistry and Organic Chemistry, Campus Sescelades, Edifici N4, C/Marcel·lí Domingo s/n, Tarragona (43007) Spain

b. Dipartimento di Scienza e Alta Tecnologia, Università degli Studi dell'Insubria, Via Valleggio, 9, Como (22100), Italy

c. Universitat Rovira i Virgili. Chemometrics, Qualimetrics and Nanosensors Group, Department of Analytical Chemistry and Organic Chemistry, Campus Sescelades, Edifici N4, C/Marcel·lí Domingo s/n, Tarragona (43007) Spain

**Corresponding author to the article: ricard.boque@urv.cat*

1. Introduction

The main biochemical change during wine alcoholic fermentation is the transformation of sugars from grape must into ethanol by the action of yeasts. In order to obtain high quality wines a close monitoring of this process is of utmost importance [1]. In the wine cellar, simple measurements such as density, pH and temperature are the main quality control parameters, which are usually measured once or twice a day to ensure a correct progression of the process and to avoid stuck and sluggish fermentations or contamination-related processes, which may lead to low quality wines [2]. If unexpected deviations occur, more exhaustive off-line laboratory analyses are needed, which involve delayed results that may not allow readjusting the process when it could still be solvable. Process Analytical Technologies (PAT) are based on the idea that quality of a product should be evaluated throughout the manufacturing process, by performing real-time measurements during processing instead of carrying out quality control measurements in the final product. PAT methodologies ensure that if a product operates under Normal Operation Conditions (NOC) it will probably meet the final quality requirements at the end of the process. PAT guidelines are founded on process understanding together with the fact that modern process analyzers can provide non-destructive measurements containing information related to biological, physical, and chemical attributes of the materials being processed [3]. Despite being developed for the pharmaceutical manufacturing, PAT have been gaining ground in the food and beverages industries [4]. In particular, when dealing with wine alcoholic fermentation monitoring and process control, the implementation of fast analytical tools, such as vibrational spectroscopy, has gained popularity over the last decades. Vibrational spectroscopy falls into the PAT guidelines as it allows getting real-time information of the process and taking corrective measures, if necessary, before obtaining the final product [5]. Among the different vibrational spectroscopy options, attenuated total reflectance mid-infrared spectroscopy (ATR-MIR) is a very valuable PAT tool for food and beverages analysis, as it is a fast and easy-to-use technique, which requires little or no sample pre-treatment [6].

To obtain the useful process information, the use of vibrational spectroscopy involves the acquisition of multivariate data and so it implies the application of multivariate statistical process control (MSPC) techniques. Among the different MSPC charts, the ones based on Principal Components Analysis (PCA) to monitor fed-batch processes are simple to represent and easy to interpret [7]. However, fed-batch processes naturally present several features, which make the modelling of NOC (Normal Operation Conditions) batches a difficult task (e.g. time-varying dynamics and uneven batch length), and different

approaches can be adopted depending on the type of process followed and the type of faults sought [8]. In batch processing, data can be represented as a three-way matrix of dimensions IxJxK (where I is the number of samples, J refer to number of variables and K is the number of time points of each batch). A decomposition into a two-way matrix of dimensions IJxK or IxJK can be applied to build multivariate PCA models. The basis of MSPC is very similar to the traditional univariate SPC methods, where the confidence limits are built based on data obtained only from NOC batches. To study the evolution of new batches, the statistical information from the PCA model is used. Particularly, Q residuals and Hotelling's T^2 values (calculated under normal distribution assumptions) are the most used statistical measures to detect irregular batches. Q residuals represent the squared perpendicular distance of a sample at a specific time point from the reduced space defined by the PCA model. They become greater when a batch deviates over time from NOC batches. Then, the irregular batch, when projected, lies outside the model, perpendicular to the NOC PCA space. In turn, Hotelling's T^2 values provide information of how far a batch is from the centre of the NOC reduced space. In this case, an abnormal batch would be positioned further away from the centre of the model as the deviation becomes more evident [9].

The combination of vibrational spectroscopy and MSPC tools to detect deviations during fed-batch processes in the food and beverages industries has already been considered, confirming the growing interest to integrate fast analytical tools and MSPC techniques into the process control line. Using FT-NIR, disturbances during the coffee roasting process were detected outside the limits of both T^2 and Q residual charts before the end of the process [10]. Similarly, faulty batches during the renneting process of milk were detected in the Q residuals chart [11]. Also, Q charts were used to detect off-specification coffee beans during storage in different packaging conditions using Raman spectroscopy [12]. However, information is very limited on the use of spectroscopic data and MSPC charts for on-line monitoring of fermentation processes in the agro-food sector to provide early indications of process deviations [13,14].

It has already been shown that ATR-MIR is suitable for real-time bioprocess monitoring [15] and particularly for monitoring industrial alcoholic fermentation processes [16,17]. In the winemaking industry, alcoholic fermentation monitoring using ATR-MIR-has been widely studied and a review on the usefulness of this technique for process control can be found elsewhere [18]. Furthermore, it has been reported that ATR-MIR can detect deviations from NOC, including sluggish fermentations and microbiological spoilage [19,20], suggesting that this tool could be used for process control. The

implementation of real-time monitoring in the cellar, together with MSPC charts, could be more efficient than performing off-line laboratory analyses, which provide delayed results and may not allow taking corrective measures when a deviation could still be solvable. Yet, the potential of MSPC charts in this field has not yet been fully investigated [21].

The aim of this study was to develop MSPC control charts as a tool for spoilage detection in the wine alcoholic fermentation process. This spoilage was promoted by inducing an additional malolactic fermentation (MLF) in some wine fermentations to evaluate the capability of the MSPC charts to detect this deviation from the normal process.

2. Materials and methods

2.1 Samples

The grape must employed to perform the small-scale fermentations (microvinifications) was obtained by the adequate dilution of a concentrated white grape must from Mostos Españoles S.A. (Ciudad Real, Spain). The diluted sugar (glucose and fructose) concentrations were 200 ± 10 g L^{-1}, in order to reproduce natural variability in samples. In addition, yeast assimilable nitrogen was adjusted by supplementation with 0.30 g L^{-1} of ENOVIT® (SPINDAL S.A.R.L Gretz Armainvilliers, France) and 0.30 g L^{-1} of Actimaxbio* (Agrovin, Ciudad Real, Spain).

Microvinifications were conducted in 500 mL conical flasks by adding 350 mL of diluted must. Each flask was inoculated with the commercial dry yeast strain *Saccharomyces cerevisiae* "E491" (Vitilevure Albaflor, YSEO, Danstar Ferment A.G., Denmark), to reach a final concentration of $3 \cdot 10^6$ CFU mL^{-1}. In total, 25 NOC microvinifications were carried out in 4 different experiments throughout the year. To emulate the variability due to a real grape ripening process, each one of the four microvinification experiments used a must with a slightly different sugar concentration. Simultaneously to the NOC experiments, 8 additional microvinifications were intentionally contaminated with a freeze-dried blend of Lactic Acid Bacteria (*Lactobacillus plantarum* and *Oenococcus oeni*) in two different concentrations, 4 x $2.5 \cdot 10^6$ and 4 x $4 \cdot 10^6$ CFU mL^{-1}, to promote malolactic fermentation at different time points of the alcoholic fermentation. Samples were coded as MLF1 and MLF2, respectively. Rehydration of the microorganisms before co-inoculation was done following the suppliers' indications.

All the microvinifications were kept under constant temperature of 18 ºC until the end of the fermentations. Both alcoholic and malolactic fermentations were controlled by routine analysis twice a day until the end of both fermentations in order to ensure the normal progress of both processes (we considered that alcoholic fermentation ended when density was under 0.995 g L^{-1} and malolactic fermentation ended when L-malic acid concentration was under 0.06 g L^{-1}). Alcoholic fermentations were controlled with density measurements with a portable densimeter (Densito2Go, Mettler Toledo, United States). Regarding to the malolactic fermentations, these were controlled by determining the L-malic acid concentration using a Y15 Analyser (Biosystems, Barcelona, Spain). pH was also continuously measured in both fermentations using a portable pH-meter with a 201 T portable electrode (7+ series portable pH-meter, XS Instruments, Italy). All the analyses were performed right after sample collection.

2.2 ATR-MIR analysis

After homogenization, 1,5 mL were collected at least once a day and centrifuged at 10000 rpm for 10 minutes, to avoid the scattering effect produced by the microorganisms present in the sample. The pellet was discarded, and the supernatant was kept in 1.5 mL eppendorfs for further analysis. Infrared measurements were performed with a portable 4100 ExoScan FTIR instrument (Agilent, California, USA), equipped with an interchangeable spherical ATR sampling interface, consisting on a diamond crystal window. Spectra were collected using our previously optimized methodology [14] over the range 4000 to 650 cm^{-1} (resolution 8 cm^{-1}; 32 scans; triplicate per sample; air-background before sample). A drop of the sample was placed on top of the crystal and the spectrum was recorded immediately afterwards. Spectra were obtained using Microlab PC software (Agilent, California, USA) and data was saved as *.spc* files. The mean of the triplicates was used in subsequent data analysis.

2.3 Multivariate statistical process control

The spectral region selected to proceed with the study was from 1309 to 1082 cm^{-1}, which according to our previous studies is the region related to the malolactic fermentation [20]. The collected data consisted of a three-way matrix containing the absorbance values at different wavenumbers (J=62), for NOC and MLF samples (I=33) and at different sampling times (K) depending on the batch. Sampling times ranged from 0 to 210 hours, when the completion of both alcoholic and malolactic fermentations was achieved. Then, a time-wise unfolding of the three-way array was performed, resulting in a matrix with dimension

IKxJ. After that, different pre-processing strategies where tested and optimized, including first and second derivatives, Savitzky-Golay smoothing and Standard Normal Variate (SNV). After spectral pre-processing, data were mean-centered.

First, a preliminary PCA model was built using only the data from the first experiment, in order to qualitatively visualize the main changes in the spectra and to detect trends in sample types (NOC and MLF). This model allowed to explore the variability of batches from the same experiment and the variability associated to the malolactic fermentation.

Next, three different strategies were applied with the unfolded, two-dimensional (IKxJ) matrix. In the first one, only NOC batches from a sole experiment were used to build a NOC PCA model (matrix of 340 rows – samples x time, and 62 columns - wavelengths). In the second strategy, NOC batches from the other experiments were added to build a new NOC PCA model including the variability among experiments. Thus, the 10 NOC samples from the previous model were used, but the matrix was augmented using 15 more NOC samples from the others three different experiments. The final NOC matrix consisted of 771 rows (NOC samples coming from the 4 experiments x time) and 62 columns (wavelengths). In both approaches, samples from all the sampling times were used. Finally, in the third strategy, eight-hour models (interval PCA models) were developed used all the NOC data. A scheme of the procedure followed for all models is shown in Figure 1.

In the three strategies, MLF samples (272 rows – samples x time, x 62 columns - wavelengths) were projected in the different NOC PCA models by calculating their scores in the NOC reduced space and using the loadings obtained from each model. The capability of the PCA models to detect a deviation during the process using the defined reduced space and the statistical performance of the MLF samples were evaluated. All models were validated by applying the Kennard-Stone algorithm [22] using half of the NOC samples in the calibration set to ensure that the whole NOC variability is represented.

For each one of three models, T^2 and Q control charts were built. A 95% Hotelling's T^2 confidence limit was calculated using the NOC calibration samples, and then NOC samples from the validation set and all MLF samples were plotted in the Hotelling's T^2 control charts, representing T^2 values vs time. Similarly, a 95% confidence limit was calculated for the Q residuals using the NOC calibration samples, and then

NOC samples from the validation set and MLF samples were projected in the Q control charts, representing in this case Q values vs time.

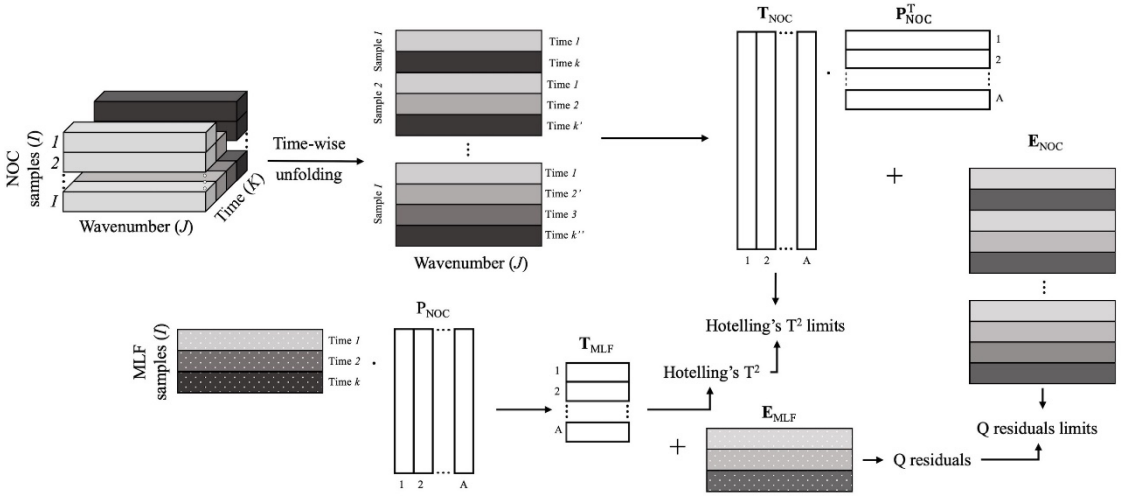

Figure 1. Scheme of the procedure applied to build the IKxJ PCA models for NOC samples and the projection of MLF samples.

All multivariate data analyses were performed using the PLS Toolbox v8.7 (Eigenvector Research Inc., Earglerock, USA) with MATLAB R2015b (The MathWorks, Natick, USA).

3. Results and discussion

3.1. Evolution of alcoholic and malolactic fermentations

As previously reported [23,24], the regions that show the greatest variability during alcoholic fermentation in the mid-infrared region are between 950 and 1500 cm^{-1}, due to sugars, acids, proteins and ethanol bonds absorption. In this region, the greatest variability associated to the biochemical transformation of sugars into ethanol and carbon dioxide is observed between 950 and 1100 cm^{-1}. However, when using the region from 950 to 1500 cm^{-1}, it was not possible to distinguish between NOC and MLF because spectral changes due to malolactic fermentation in this region were hidden by spectral changes corresponding to the main process (alcoholic fermentation) (data not shown). For this reason, to focus on the malolactic fermentation process, we used the region between 1309 to 1082 cm^{-1}, which maximised the differences between alcoholic and malolactic fermentations.

The optimized pre-processing used was first derivative (1st order polynomial) with Savitzky-Golay smoothing through 15 points, SNV and mean-center. A preliminary PCA model was built only using samples from a single experiment (consisting on 10 NOC and 8 MLF batches), attempting to screen different behaviours between NOC and MLF samples. The number of principal components used for this purpose was optimized to 2 PCs, to well-define alcoholic fermentation and avoid overfitted models. As it can be observed in Figure 2, the first principal component (98.61% explained variance) follows the trend of alcoholic fermentation kinetics, as shown in our previous work [20]. From the second principal component (accounting for only a 1.04% of the total variability), a difference can be observed between NOC and MLF samples from hours 60-80 until the end of the process. It must be taken into account that the greatest variability in the spectra is due to the alcoholic fermentation, as it involves the transformation of sugars into ethanol from an initial concentration of 200 g L^{-1}. On the other hand, at the beginning of malolactic fermentation, malic acid concentration is only around 2 g L^{-1} and the variability in the signal is much lower. Moreover, even though the second bioprocess does not interfere in the first bioprocess, sugars' and acids' bonds absorb in the same regions of the spectra, which makes it hard to detect MLF deviations. Figure 2 shows that differences between NOC and MLF start to be noticeable 80 hours after the beginning of the process, and a separation trend can be appreciated between 40 and 80 hours.

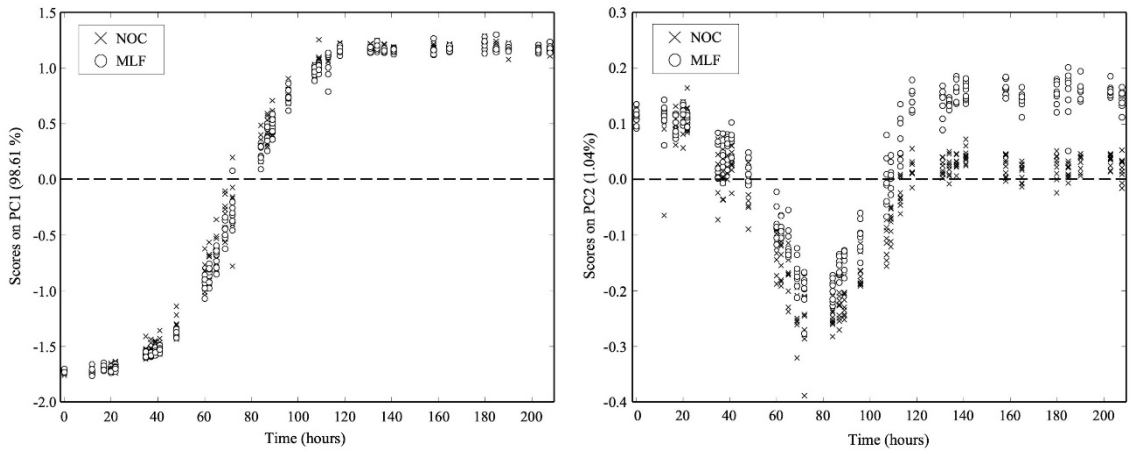

Figure 2. Scores for PC1 (left) and PC2 (right) for a singles batch fermentation.

3.2 MSPC charts for monitoring fermentations

3.2.1 Single experiment strategy

The MSPC charts used in this strategy are based on the Q and T^2 statistics. NOC samples used to build the PCA in section 3.1 were also used to build a single experiment NOC PCA model (matrix 340x62). The scores of this model were used to calculate the T^2 95% confidence limit, and the residual matrix of

this model was used to calculate the Q-residuals 95% confidence limit. Q and T^2 vs time control charts are shown in Figure 3 for the 10 NOC and the 8 MLF batches (4 MLF1 and 4 MLF2). In both charts, NOC samples lie below the 95% confidence limit during the main course of the alcoholic fermentations. In contrast, MLF samples in the Q control chart show a significant difference from NOC samples from 80 hours onwards, as it was already observed in the PCA scores plot (Figure 2, section 3.1). On the other hand, all MLF samples lie below the confidence limits in the T^2 chart. Nevertheless, MLF samples exhibit a trend of higher T^2 values with respect to NOC samples from hour 110. These higher values could be explained because malolactic fermentation at this time is almost finished, and the distance to the centre of the model increases but not significantly, from a statistical point of view.

The fact that MLF samples are distinguishable from NOC samples in the Q chart but not in the T^2 chart is a reasonable result because the enormous variability in the spectra due to alcoholic fermentation (especially between hours 70 and 90 when tumultuous fermentation takes place (in figure 2, from hour 40 to 120, when sugar consumption is at its fastest rate) hampers the possibility to establish a confidence limit to differentiate the samples. It is important to remark that, despite the fact that a different trend between MLF and NOC samples can be seen after >100h, all samples fall under the confidence limit because of the mentioned variability among samples between hours 70 and 90h. Furthermore, malolactic fermentation evolution in the spectrum is jumbled with alcoholic fermentation, explaining the difficulty in finding the differentiation.

This methodology was validated by applying the Kennard-Stone algorithm. NOC samples were split using 50% of them to build the model (calibration set) and the remaining 50% for validation. Q values from the validation NOC samples were under the new Q residual confidence limit. Similarly, MLF samples showed a similar behaviour as in the model built with all NOC samples.

This time-wise unfolding approach is proposed as an alternative to *IxJK* batch-wise unfolding [8], were the exact same number of sampling times is required in order to project new suspected samples. We previously reported the use of a time-wise approach to detect sluggish alcoholic fermentations [14]. Here, any spectrum from a MLF batch can be projected onto model, and the model is able to determine if the sample is under or above the confidence limit, with no need to neither follow its complete alcoholic fermentation, nor to have the same exact amount of sampling points during the process. To confirm this idea, MLF samples from a single time point (hour 119), which were above the Q confidence limit, were

projected solely and, as samples are independent of the time, they were placed above the Q confident limit.

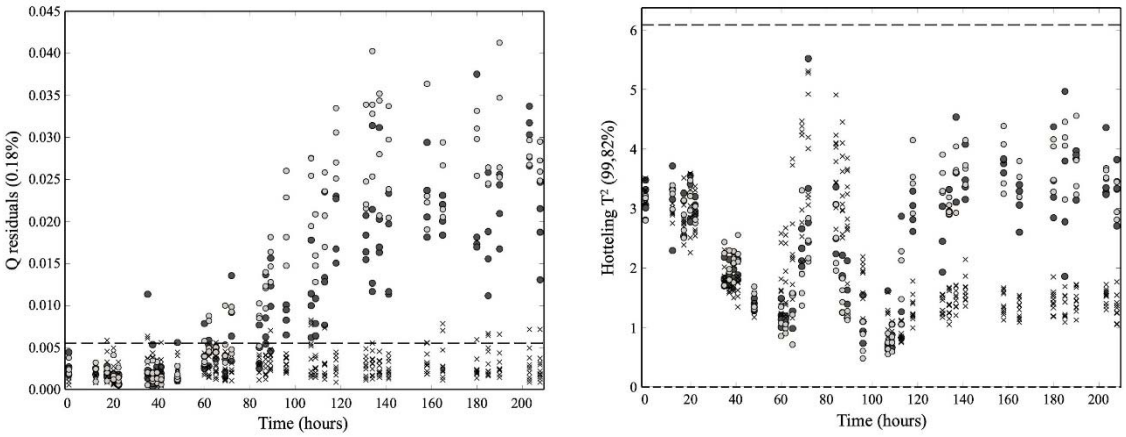

Figure 3. Q and T2 charts for a single experiment. Symbols: (x) NOC, (●) MLF1 (○) MLF2.

3.2.2 Multiple experiment strategy

To confirm the hypothesis that it is not necessary to have the same sampling times and number of sampling points, three different experiments consisting of 15 additional NOC batches were added to the model. In every experiment, sampling was performed at similar, but not exactly, the same time points. This methodology perfectly agrees with the typical control timing in a winery, where the fermentation control is performed usually once or twice a day and not in each fermentation tank at the same time. In this case, as different NOC batches with different initial sugar concentrations (which implies different sugar consumption rates) were used (matrix dimensions of 771x62), the model was validated following the same procedure as in the single experiment model, assuring that NOC samples from all the experiments were included in both sets. As it can be observed in Figure 4, NOC validation samples are generally under the 95% confidence limit in both Q and T control charts, assuring the validation of the model. In this model the trend observed in the Q control chart for the MLF samples is similar as in the previous PCA model when using a single experiment (section 3.2), with a separation from hour 80 onwards. For the T^2 control chart, despite exhibiting the same trend observed in the model from section 3.2, MLF samples are now statistically different from hour 120 until the end of the process. This may be explained because as more NOC samples are included in the NOC model, alcoholic fermentation variability is better described, and the model is able to detect the differences among NOC samples and MLF, which can now be statistically differentiated after hour 120.

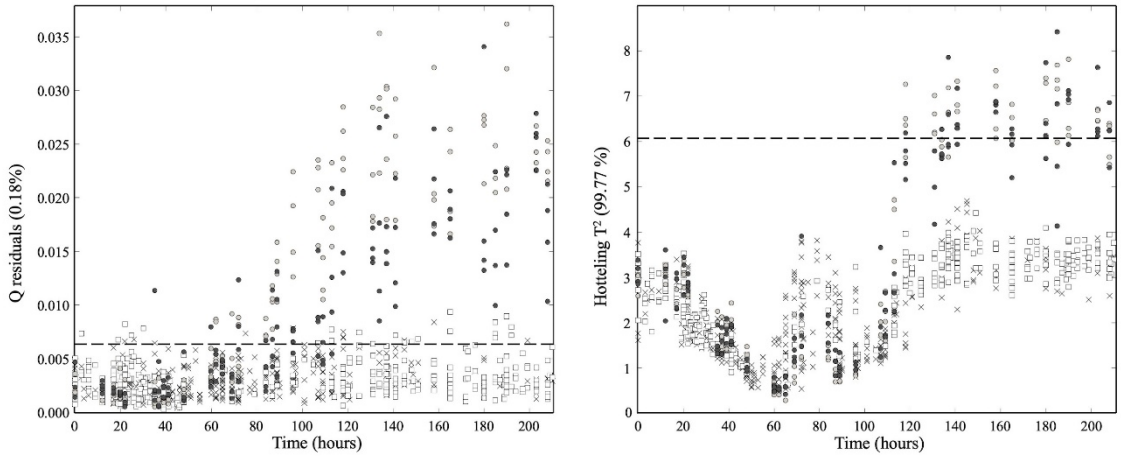

Figure 4. Q and T2 charts for all the experiments. (x) Calibration NOC samples, (☐) validation NOC samples, (⬤) MLF1 (◯ MLF2.

As in the single experiment model, samples are independent of the sampling time and the full trajectory of the batch is not needed. Any single MLF spectrum can be projected into the model and this will be able to determine if the sample is statistically different in both Q and T^2 control charts. In other words, MLF samples will appear in the same position in the Q and T^2 charts as it happened when all the MLF samples were projected, regardless of the sampling times available.

3.2.3 Interval models' strategy

As it could be inferred from the T^2 control chart in Figure 4, during tumultuous fermentation (in figure 2, from hour 40 to 120), higher T^2 values are observed. It would then be useful to build specific models for certain time intervals, as more accurate confidence limits could be stablished, especially for Hotelling's T^2. An 8-hour time interval was defined, because this period of time would be sufficient to take corrective measures in a winery and also, the changes in the matrix during this period would not affect the final product quality.

In this approach, all NOC and MLF matrix (771x61) was divided into 8-hour time-intervals, and PCA models were built for each interval until the separation of MLF samples. Matrixes of different sizes were used depending on the number of samples available at each time-interval. With the T^2 control charts, no statistical separation was achieved, showing that T^2 statistics does not represent a useful way to detect deviations. The model built with the time interval between 65 and 72 hours (Figure 5) shows a MLF

separation trend. This time interval model could be useful as an alert indicator before all MLF batches are completely separated, to foresee a spoilage at early stages of the malolactic fermentation. In this case, the Q values of MLF1 samples are slightly smaller than the ones of MLF2, as MLF2 samples have a higher concentration of LAB (higher L-malic acid consumption rate). The complete statistical separation in the Q chart was obtained in the model between 81 and 88 hours. Models were also built for subsequent time intervals, in order to assure that the separation is consistent until the end of the malolactic fermentation. Our results show that a malolactic fermentation detection threshold can be established as an indicator that a deviation is arising at the 65-72h interval, when 40-50% of this bioprocess has taken place. At this point, additional measures should be taken to readjust the principal process (alcoholic fermentation) and to avoid having a worse situation which could lead to wines with organoleptic defects or even worse, the loss of a whole vintage.

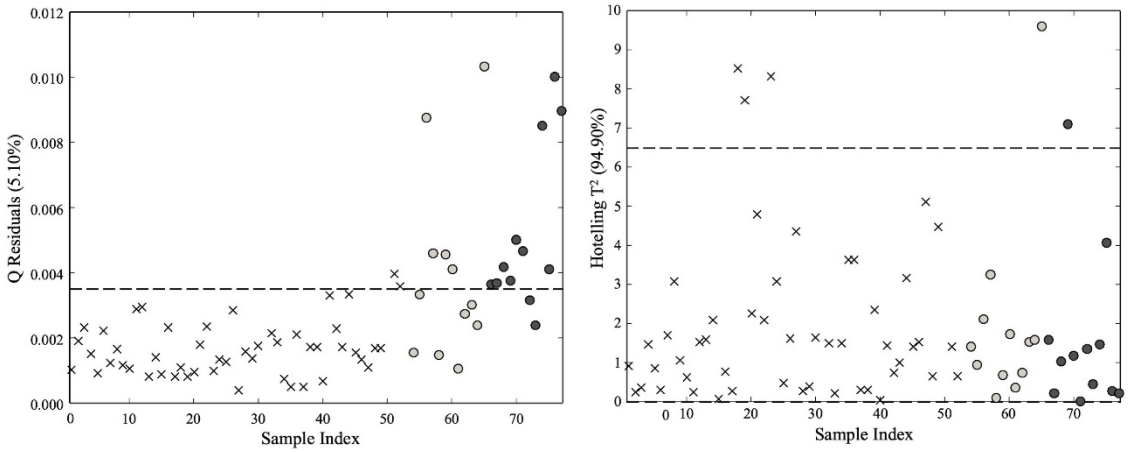

Figure 5. Time interval 65-72 hours. (X) NOC samples, (◯) MLF1, (●) MLF2.

4. Conclusions

In the best of our knowledge, this is the first time that Q residuals and Hotelling's T^2 control charts are used for the detection of an unwanted malolactic fermentation during alcoholic fermentation in wine based on ATR-MIR spectroscopic data. It was demonstrated that a specific signal pretreatment (e.g. batch alignment) is not required since typical year-to-year variability is considered in the global model. Also, using specific interval models improves the performance of the statistical detection of malolactic fermentation in the Q residual control chart. In conclusion, the different approaches here presented have

297 the potential to be used in the oenological field, as an early detection of fermentation problems based on
298 MSPC charts,

299

300 **Acknowledgements**

301 We thank the Spanish Ministry of Economy and Competitiveness and the European Regional
302 Development Fund (FEDER) (project AGL2015-70106-R, AEI-FEDER,UE) for the financial support
303 given. Cavaglia, J. would also like to thank the Catalan Agency for Management of University and
304 Research Grants (AGAUR) for the FI grant (FI_B100154).

305

306 **REFERENCES**

307 [1] P. Ribéreau-Gayon, D. Dubourdieu, B. Donèche, A. Lonvaud, Handbook of Enology Volume 1
308 The Microbiology of Wine and Vinifications 2 nd Edition, 2nd Editio, 2006.
309 doi:10.1002/0470010363.fmatter.

310 [2] L.F. Bisson, Stuck and sluggish fermentations, Am. J. Enol. Vitic. 50 (1999) 107–119.

311 [3] Guidance for Industry PAT — A Framework for Innovative Pharmaceutical Development,
312 Manufacuring, and Quality Assurance, FDA Off. Doc. (2004) 16.

313 [4] M. Jenzsch, C. Bell, S. Buziol, F. Kepert, H. Wegele, C. Hakemey, Trends in Process Analytical
314 Technology: Present state in bioprocessing, in: B. Kiss, U. Gottschal, M. Pohlscheidt (Eds.), New
315 Bioprocess. Strateg. Dev. Manuf. Recomb. Antibodies Proteins, 1st Editio, Springer International
316 Publishing, Switzerland, 2018: pp. 211–252.

317 [5] F. Van Den Berg, C.B. Lyndgaard, K.M. Sørensen, S.B. Engelsen, Process Analytical
318 Technology in the food industry, Trends Food Sci. Technol. 31 (2013) 27–35.
319 doi:10.1016/j.tifs.2012.04.007.

320 [6] P. Roychoudhury, L.M. Harvey, B. McNeil, The potential of mid infrared spectroscopy (MIRS)
321 for real time bioprocess monitoring, Anal. Chim. Acta. 571 (2006) 159–166.
322 doi:10.1016/j.aca.2006.04.086.

323 [7] P. Nomikos, J.F. MacGregor, Multi-way partial least squares in monitoring batch processes,

Chemom. Intell. Lab. Syst. 30 (1995) 97–108. doi:10.1016/0169-7439(95)00043-7.

[8] J. Camacho, J. Picó, A. Ferrer, The best approaches in the on-line monitoring of batch processes based on PCA: Does the modelling structure matter?, Anal. Chim. Acta. 642 (2009) 59–68. doi:10.1016/j.aca.2009.02.001.

[9] P. Nomikos, J.F. MacGregor, Monitoring batch processes using multiway principal component analysis, AIChE J. 40 (1994) 1361–1375. doi:10.1002/aic.690400809.

[10] T.A. Catelani, J.R. Santos, R.N.M.J. Páscoa, L. Pezza, H.R. Pezza, J.A. Lopes, Real-time monitoring of a coffee roasting process with near infrared spectroscopy using multivariate statistical analysis: A feasibility study, Talanta. 179 (2018) 292–299. doi:10.1016/j.talanta.2017.11.010.

[11] S. Grassi, L. Strani, E. Casiraghi, C. Alamprese, Control and Monitoring of Milk Renneting Using FT-NIR Spectroscopy as a Process Analytical Technology Tool, Foods. 8 (2019) 405. doi:10.3390/foods8090405.

[12] G.F. Abreu, F.M. Borém, L.F.C. Oliveira, M.R. Almeida, A.P.C. Alves, Raman spectroscopy: A new strategy for monitoring the quality of green coffee beans during storage, Food Chem. 287 (2019) 241–248. doi:10.1016/j.foodchem.2019.02.019.

[13] P. Jørgensen, J.G. Pedersen, E.P. Jensen, K.H. Esbensen, On-line batch fermentation process monitoring (NIR) - Introducing “biological process time,” J. Chemom. 18 (2004) 81–91. doi:10.1002/cem.850.

[14] J. Cavaglia, B. Giussani, M. Mestres, M. Puxeu, O. Busto, J. Ferré, R. Boqué, Early detection of undesirable deviations in must fermentation using a portable FTIR□ATR instrument and multivariate analysis, J. Chemom. (2019) 1–11. doi:10.1002/cem.3162.

[15] J.J. Roberts, A. Power, J. Chapman, S. Chandra, D. Cozzolino, Vibrational Spectroscopy Methods for Agro-Food Product Analysis, in: Compr. Anal. Chem., 2018: pp. 51–68. doi:10.1016/bs.coac.2018.03.002.

[16] E.L. Veale, J. Irudayaraj, A. Demirci, An on-line approach to monitor ethanol fermentation using FTIR spectroscopy, Biotechnol. Prog. 23 (2007) 494–500. doi:10.1021/bp060306v.

[17] K.C.S. Rodrigues, J.L.S. Sonego, A. Bernardo, M.P.A. Ribeiro, A.J.G. Cruz, A.C. Badino, Real-

Time Monitoring of Bioethanol Fermentation with Industrial Musts Using Mid-Infrared Spectroscopy, Ind. Eng. Chem. Res. 57 (2018) 10823–10831. doi:10.1021/acs.iecr.8b01181.

[18] R. Dambergs, M. Gishen, D. Cozzolino, A review of the state of the art, limitations, and perspectives of infrared spectroscopy for the analysis of wine grapes, must, and grapevine tissue, Appl. Spectrosc. Rev. 50 (2015) 261–278. doi:10.1080/05704928.2014.966380.

[19] A. Urtubia, J. Ricardo Pérez-Correa, F. Pizarro, E. Agosin, Exploring the applicability of MIR spectroscopy to detect early indications of wine fermentation problems, Food Control. 19 (2008) 382–388. doi:10.1016/j.foodcont.2007.04.017.

[20] J. Cavaglia, D. Schorn-García, B. Giussani, J. Ferré, O. Busto, L. Aceña, M. Mestres, R. Boqué, ATR-MIR spectroscopy and multivariate analysis in alcoholic fermentation monitoring and lactic acid bacteria spoilage detection, Food Control. 109 (2020) 106947. doi:10.1016/j.foodcont.2019.106947.

[21] G. Hernández, R. León, A. Urtubia, Detection of abnormal processes of wine fermentation by support vector machines, Clust. Comput. 19 (2016) 1219–1225. doi:10.1007/s10586-016-0594-5.

[22] R.W. Kennard, L.A. Stone, Technometrics Computer Aided Design of Experiments, Technometric. 11 (1969) 137–148.

[23] D. Cozzolino, C. Curtin, The use of attenuated total reflectance as tool to monitor the time course of fermentation in wild ferments, Food Control. 26 (2012) 241–246. doi:10.1016/j.foodcont.2012.02.006.

[24] Z. Wu, E. Xu, J. Long, Y. Zhang, F. Wang, X. Xu, Z. Jin, A. Jiao, Monitoring of fermentation process parameters of Chinese rice wine using attenuated total reflectance mid-infrared spectroscopy, Food Control. 50 (2015) 405–412. doi:10.1016/j.foodcont.2014.09.028.